

Study of Temperature Difference and Current Distribution in Parallel-Connected Cells at Low Temperature

Sara Kamalishahroudi, Jun Huang, Zhe Li, Jianbo Zhang

Abstract—Two types of commercial cylindrical lithium ion batteries (Panasonic 3.4 Ah NCR-18650B and Samsung 2.9 Ah INR-18650), were investigated experimentally. The capacities of these samples were individually measured using constant current-constant voltage (CC-CV) method at different ambient temperatures (-10°C, 0°C, 25°C). Their internal resistance was determined by electrochemical impedance spectroscopy (EIS) and pulse discharge methods. The cells with different configurations of parallel connection NCR-NCR, INR-INR and NCR-INR were charged/discharged at the aforementioned ambient temperatures. The results showed that the difference of internal resistance between cells much more evident at low temperatures. Furthermore, the parallel connection of NCR-NCR exhibits the most uniform temperature distribution in cells at -10°C, this feature is quite favorable for the safety of the battery pack.

Keywords—Batteries in parallel connection, internal resistance, low temperature, temperature difference, current distribution.

I. INTRODUCTION

THE lithium ion batteries are one of the most widely used power sources in hybrid electrical vehicles (HEVs) and battery electrical vehicles (BEVs) for their high specific energy and power [1]. To achieve the high power in vehicles the cells are connected in parallel, series or parallel-series to constitute a pack. The uniform distribution of temperature and current in a battery pack is a key factor that guarantees battery performance, safety and lifetime. The imbalance among cells can be caused by several factors, including external causes like variations in contact resistance of the cell or internal ones such as variations in cell quality [2].

In parallel connected cells, current distribution in a battery pack is determined by cells' internal resistance, which depends on several factors such as battery temperature, its active material contents and the state of charge [3]. At very low temperatures, the sluggish nature of charge transfer reactions leads to a significant increase in battery internal resistance [4]. Due to inverse relation between irreversible heat generation rates and resistance ($Q = U^2/R$), one can expect higher temperature growth in low-resistance battery in parallel

configuration. Then, this quick temperature rise will work on the resistance difference and current distribution in return. Therefore, the purposes of this study are to investigate the current distribution in parallel connected cells and to evaluate the effect of temperature on the current distribution by considering their internal resistance.

II. BACKGROUND

According to former studies, battery temperature, current density and its state of charge (SoC) have important effects on its lifetime [5]. To estimate the distribution of current in multi-cell connection, a circuit based model has been proposed [6]. It has been observed, when the battery cells are connected in parallel, the internal resistance mismatching between cells can accelerate battery capacity fading [7]. It is also indicated that the current density distribution and local SoC differences due to temperature gradient leads to cell degradation [8]. In addition, after repetitive charge/discharge of battery pack, the cells are found to deviate from their uniformity gradually [9] that can extremely affect battery pack safety and reliability.

As mentioned before, the current distribution is determined by the cell resistance. This study intends to investigate the current distribution in different temperatures for parallel connected cells to explore the low temperature effects on current distributions. In the first part, the capacity and internal resistance of single cell were measured. Then, in the second part, the parallel connections of the cells at low temperature were investigated in terms of current and temperature distributions.

III. EXPERIMENTAL

Experiments to parameterize the battery capacity and internal resistance for two types of batteries, Panasonic NCR 18650B 3.4 Ah (green) and Samsung INR18650 2.9 Ah (blue), were conducted using a MACCOR 4000 source measure unit to control the current and voltage and a GDJW-225 thermal chamber to regulate the environment temperature of the cells. The initial temperature of the battery is assumed to be isothermal, and the AUTOLAB system measured the battery internal resistance, by electrochemical impedance spectroscopy (EIS) method.

The capacity of each cell was measured by cycling the battery cells at low C-rate (C/3) at different temperatures (-10°C, 0°C and 25°C) using CC-CV protocol. After determining the battery capacities, their internal resistances were measured, using two methods explained below.

S. Kamalishahroudi, master student, J. Huang, Ph.D. student, and Zhe Li, assistant professor, are with the Department of Automotive Engineering, State Key Laboratory of Automotive Safety and Energy, Tsinghua University, Beijing 100084, P. R. China (e-mail: sarakamali61@gmail.com, huangjun12@mails.tsinghua.edu.cn, lizhe02@mails.tsinghua.edu.cn).

J. Zhang, professor, is with the Department of Automotive Engineering, State Key Laboratory of Automotive Safety and Energy, Tsinghua University, Beijing 100084, P. R. China (phone: +86-10-62786918 e-mail: jbzhang@tsinghua.edu.cn).

In Pulse discharge method [10], the battery was soaked at room temperature (25°C) for one hour to reach thermal balance. Then the previously-fully-discharged battery was charged on the whole SoC range using CC-CV protocol, to finally reach 4.2 V with the cut-off current of 50 mA. After one hour rest, the battery was discharged by 1C rate with the step of 10% SoC, each step followed by one hour rest. This process was repeated until the 3 V minimum was reached. The EIS method which was performed at three SoCs (0, 0.5 and 1). In this method the battery terminals were connected to the AUTOLAB system that was controlled by a computer. For each open circuit voltage (OCV), a small alternative current (AC) with different frequencies from 100 kHz to 0.1 HZ were applied to the battery and the voltage responses were recorded by the computer.

After obtaining the batteries capacity and internal resistance, the batteries were connected in parallel configuration. In this part, a thermocouple and a Hall-effect current sensor were equipped to each connected cells to measure temperature and current (Fig. 1).

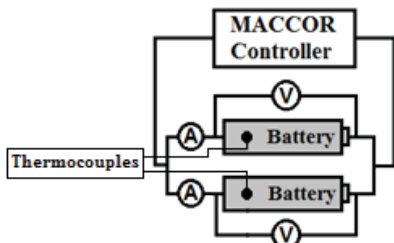


Fig. 1 Schematic of the battery connections for experiments

The connected cells, were charged by a total current of 4 A at $T=25^\circ\text{C}$ to get 4.2 V by 50 mA cut-off current. Then the connected batteries were discharged in different temperatures (-10, 0, 25°C) using 6 A current as the discharge load current.

IV. RESULTS AND DISCUSSIONS

A. Specifications of the Single Cell: Capacity and Resistance

In the first step, the capacity of each battery was measured in three different temperatures by CC-CV protocol. The results are shown in Table I.

TABLE I
THE RESULTS OF CAPACITY MEASUREMENTS IN DIFFERENT TEMPERATURE

Samples	Capacity (Ah)		
	25 °C	0 °C	-10 °C
N1	3.1	2.65	2.22
N2	3.13	2.66	2.3
I1	2.91	2.45	2.26
I2	2.89	2.44	2.26

For the internal resistance measurement by pulse discharge method, the experimental data were separated in two parts. The first part is considered to be the R_s , which consisted of battery Ohmic resistance and its charge transfer resistance. The second part is corresponded to the RC pairs that attributed to the ion diffusion resistance inside the battery. To calculate diffusion

resistance in the RC pairs, the relaxation part of voltage curve was fitted using MICROCAL ORIGIN [11] software after each discharge pulse (Fig. 2).

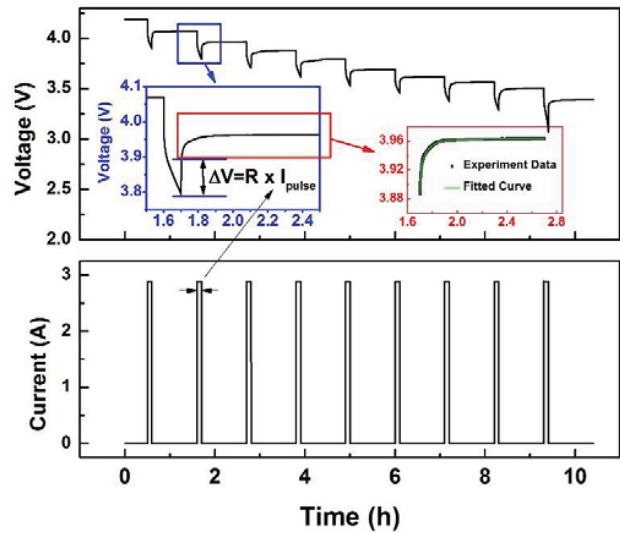


Fig. 2 Pulse discharge method for battery internal resistance calculation

For RC pair fitting, a two-term equation was employed which gives good fitting results. The fitting equation is shown below:

$$V_{relax} t_r = IR_s + IR_1 \left(1 - \exp \left(-\frac{t_{pulse}}{R_1 C_1} \right) \right) + IR_2 \left(1 - \exp \left(-\frac{t_{pulse}}{R_2 C_2} \right) \right) \quad (1)$$

where t_{pulse} the discharge is pulse time duration and t_r is the voltage recovery time.

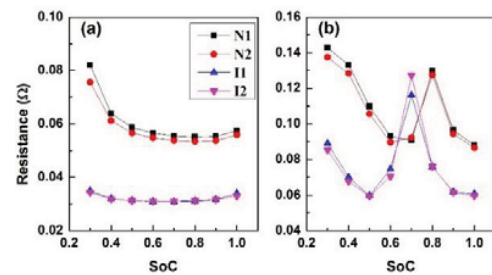


Fig. 3 (a) The Ohmic and charge transfer resistance (R_s) and (b) total resistance R_s and diffusion resistance

As it can be seen in the Fig. 3 the resistance of NCR type is higher than INR type at room temperature, and the resistance difference between two types of cells is not significant. In terms of the relationship between resistance and SoC, in the NCR type, the N1 has higher resistance at all SoCs, while in INR type, the I1 is higher at first but after $\text{SoC}=0.7$, the I2 climbed higher. The resistance differences between NCR cells are higher than INR cells.

In the second method, the EIS data were fitted using

(LR(QR)(QR)W), circuit model by ZSimp-Win software (Fig. 4). Three noticeable results are: (1) the resistances of NCR batteries were higher than INR batteries at low temperatures, (2) the internal resistance difference between similar type cells was much more evident at low temperatures, (3) there was a remarkable resistance difference between two types of batteries at low temperatures. This conclusions will be reinforced by even more evidences when analyzing the test results of the parallel connected batteries, which are discussed in next section.

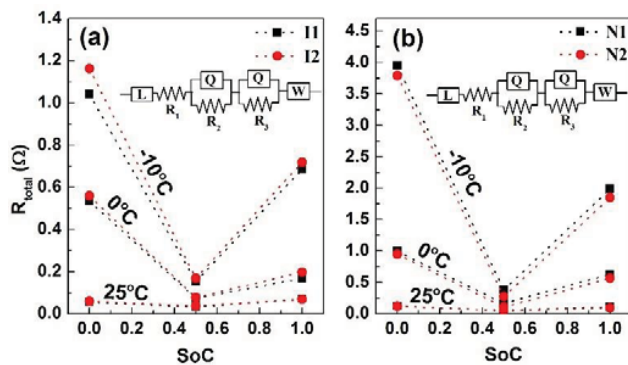


Fig. 4 Extracted resistance ($R_{\text{total}}=R_1+R_2+R_3$) of battery from EIS test (a) INR type (b) NCR type battery. The inset shows the fitted curve of equivalent electrical circuit on experimental data (The dotted lines were drawn to determine the temperature)

B. Battery Cells Investigations in Different Connection Configurations

The current and temperature distributions of the cells in charging protocol were shown in Fig. 5. As expected, in each pair of batteries, the battery with low internal resistance passes through much amount of current. According to this plot, the current and temperature distributions of NCR-NCR are much more uniform than other types, although according to Fig. 3 there was a noticeable difference between cells resistance compared with INR type (Figs. 5 (a) and (b)). These effects can be attributed to the materials of the batteries. It can be concluded that the electrochemical uniformity cannot guarantee thermal uniformity of the cells in a pack and vice versa. The maximum temperature is attained at the end of constant current (CC) stage of the battery charge protocol, but in NCR-NCR connection, the maximum temperature occurs earlier than that of other types. When two connected cells are different (Fig. 5 (c)), due to higher resistance differences between them, the current and temperature distributions are more significant. During the CV stage, the current difference between cells in NCR-INR type is more obvious than the other two types of connections. The charging duration of the parallel NCR-INR connection is somewhere between that of two other types.

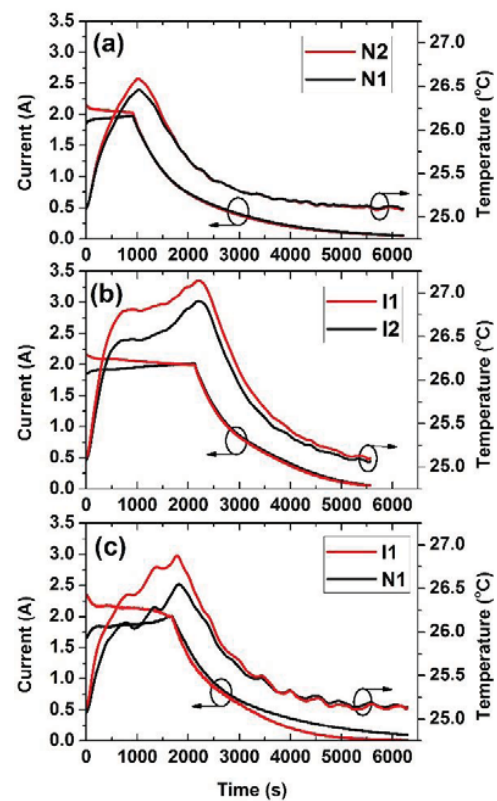


Fig. 5 Charging the connected batteries (a) parallel NCR-NCR, (b) parallel INR-INR and (c) parallel INR-NCR. The insets show the temperature change of the batteries by time

As it can be seen in Fig. 5, the temperature is higher in the low resistance cell during the charging cycle. The operation at low temperatures can lead to lithium plating during cycling, while operation at high temperatures accelerates the growth of solid electrolyte interface (SEI) layer. Both of these phenomena can lead to faster cycle life degradation [12], which increases battery internal resistance. During the CV stage of charge protocol (Fig. 5 (c)) there is a gap between current diagrams of NCR-INR cells. In fact it refers to their big resistance difference compared with other types that leads to their high SoC difference (much current goes through the lower resistance cell). The current distribution of the NCR-NCR connection reaches the full charge state earlier than other connections in CC stage of charge protocol (Fig. 5 (a)).

In discharge process, the noticeable thing is the effect of low temperature. As it is clear in Fig. 6, the NCR-NCR connections showed much uniform current distribution and temperature differences at low temperatures, because of their low resistance differences at this temperature. For NCR-NCR connection, there is one intersection of the current curve at 25 °C because of their higher sensitivity of resistance to low temperature than other types, while for INR-INR there are two intersections at 25°C and 0°C. For NCR-INR, due to high resistance difference between these two types of cells at low temperatures there is no intersection at -10°C and 0°C.

The temperature distribution shows high difference for

NCR-INR type. It can be interpreted with reparative driving cycles, where the non-uniform ageing effect on each cell increases the internal resistance difference between them. And the result of this effect will increase the temperature distribution non-uniformity in the pack.

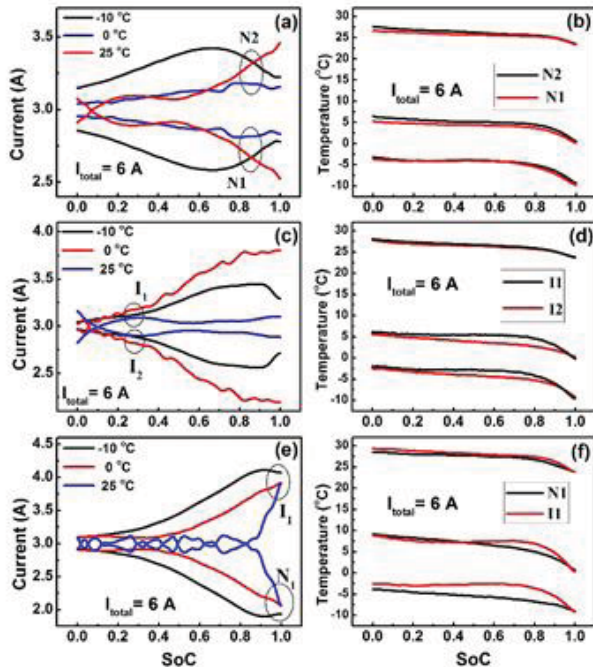


Fig. 6 Current variation of the parallel connected batteries during discharge for (a) NCR-NCR, (c) INR-INR and (e) INR-NCR. The temperature variation during the discharge process for (b) NCR-NCR, (d) INR-INR and (f) INR-NCR

V. CONCLUSION

In this study, two different types of battery, Panasonic NCR18650B (Green) and Samsung 18650 (Blue), in different parallel configurations (NCR-NCR, INR-INR and INR-NCR) have been investigated for their temperature and current investigation during cycling at three different temperatures. The results showed that the NCR-NCR connection has better uniformities than the other types, especially at low temperatures.

The resistance and resistance variation, which both have direct effects on temperature distributions between parallel connected cells, were investigated in charge protocol. Although the NCR-NCR connection had more resistance difference but it exhibited a more uniform temperature distribution. It can be concluded that the electrochemical uniformity can't guarantee thermal uniformity and vice versa. For the NCR-NCR which had higher resistance at low temperatures, the discharge current diagram didn't show sufficient intersection at low temperatures. The INR-INR exhibited interference between currents of the cells at zero centigrade. The maximum amount of current distribution difference and temperature distribution non-uniformity between cells were increased by using different cells in parallel connection. The obtained results can be applied

to the estimation of properties and optimization of cells in battery pack.

ACKNOWLEDGMENT

This study was supported by the National Natural Science Foundation of China under the grant number of 51207080, and the China Post-doctoral Science Foundation under the Grant number of 2012M510436.

REFERENCES

- [1] V. Srinivasan and C. Y. Wang, "Analysis of Electrochemical and Thermal Behavior of Li-Ion Cells," *Journal of the Electrochemical Society*, vol. 150, p. A98, 2003.
- [2] J. Kim and B. H. Cho, "Screening process-based modeling of the multi-cell battery string in series and parallel connections for high accuracy state-of-charge estimation," *Energy*, vol. 57, pp. 581–599, 2013.
- [3] M. Dubarry, N. Vuillaume, and B. Y. Liaw, "From single cell model to battery pack simulation for Li-ion batteries," *J. Power Sources*, vol. 186, pp. 500–507, 2009.
- [4] A. N. Jansen, D. W. Dees, D. P. Abraham, K. Amine, and G. L. Henriksen, "Low-temperature study of lithium-ion cells using a LiySn micro-reference electrode," *J. Power Sources*, vol. 174, pp. 373–379, 2007.
- [5] P. Ramadass, B. Haran, R. White, and B. N. Popov, "Mathematical modeling of the capacity fade of Li-ion cells," *J. Power Sources*, vol. 123, pp. 230–240, 2003.
- [6] J. Zhang, S. Ci, H. Sharif, and M. Alahmad, "An enhanced circuit-based model for single-cell battery," in *Conference Proceedings - IEEE Applied Power Electronics Conference and Exposition - APEC*, 2010, pp. 672–675.
- [7] R. Gogoana, M. B. Pinson, M. Z. Bazant, and S. E. Sarma, "Internal resistance matching for parallel-connected lithium-ion cells and impacts on battery pack cycle life," *J. Power Sources*, vol. 252, pp. 8–13, 2014.
- [8] M. Fleckenstein, O. Bohlen, M. A. Roscher, and B. Bäker, "Current density and state of charge inhomogeneities in Li-ion battery cells with LiFePO₄ as cathode material due to temperature gradients," *Journal of Power Sources*, vol. 196, pp. 4769–4778, 2011.
- [9] D. Andrea, *Battery Management Systems for Large Lithium Ion Battery Packs*. 2010, p. 300.
- [10] H. E. Perez, J. B. Siegel, X. Lin, and A. G. Stefanopoulou, "Parameterization and Validation of an Integrated Electro-Thermal Cylindrical LFP Battery Model," *ASME 2012 5th Annu. Dyn. Syst. Control Conf.*, pp. 1–10, 2012.
- [11] Available: www.originlab.com.
- [12] R. Gogoana, "Internal Resistance Variances in Lithium-Ion Batteries and Implications in Manufacturing," Available online at: <http://hdl.handle.net/1721.1/74917>.